WILEY-VCH

Critical Role of Electron-Donating Thiophene Group on the Thermomechanical Property of Donor-Acceptor Semiconducting Polymers

Song Zhang, Michael U. Ocheje, Lifeng Huang, Luke Galuska, Zhiqiang Cao, Shaochuan Luo, Dakota Ehlenberg, Renée Goodman, Dongshan Zhou, Yi Liu, Yu-Cheng Chiu, Jason D. Azoulay, Simon Rondeau-Gagné∗ and Xiaodan Gu∗

School of Polymer Science and Engineering, Center for Optoelectronic Materials and Device, The University of Southern Mississippi
Hattiesburg, MS 39406, USA
E-mail: xiaodan.gu@usm.edu

Michael U. Ocheje, Renée Goodman, Prof. Simon Rondeau-Gagné
Department of Chemistry and Biochemistry
University of Windsor
Ontario, N9B3P4, Canada
Email: simon.rondeau-gagne@uwindsor.ca

Shaochuan Luo, Prof. Dongshan Zhou
Department of Polymer Science and Engineering, School of Chemistry and Chemical Engineering
Nanjing University
Nanjing 210093, China

Dr. Yi Liu
The Molecular Foundry
Lawrence Berkeley National Laboratory
Berkeley, CA 94720, United States

Prof. Yu-Cheng Chiu
Department of Chemical Engineering
National Taiwan University of Science and Technology
Taipei 106, Taiwan

1

Abstract: Organic semiconducting polymers are promising candidates for stretchable electronics for their mechanical compliance. Despite the wide spread application for Donor-Acceptor type conjugated polymers in electronic devices due to recent boost in electronic property, the effect of the electron-donating thiophene group on the thermomechanical property of conjugated polymers has not been carefully studied. Here, we investigated thin film mechanical property for diketopyrrolopyrrole (DPP)-based conjugated polymers with varying electron donating groups by changing the number of isolated thiophene moieties and the size of fused thiophene rings in the polymer backbone. Interestingly, we found that the thiophene unit acted as an anti-plasticizer, which resulted in increased glass transition temperature (T_g) of the polymer backbone, and consequently elastic modulus of the respective DPP polymers. Regarding the deformability, the DPP polymer with isolated thiophene building blocks showed impressive stretchability up to 50%, measured by pseudo-free standing tensile test. Detailed morphological study for DPP films by atomic force microscopy, optical spectroscopy and X-ray scattering suggested that all samples showed similar semicrystalline morphology. This anti-plasticization effect also exists in para-azaquinodimethane (p-AQM)-based conjugated polymers, indicating that this can be a general trend for various conjugated polymer systems. Using the knowledge gained above, a new DPP-based polymer with increased alkyl side chain density through attaching alky chains to the thiophene unit was engineered. The new DPP polymer demonstrated a record low glass transition temperature, high stretchability up to 35%, and 50% lower in elastic modulus compared to the reference polymer that without side-chain decorated on the thiophene unit. This work can provide a general design rule for making low T_g conjugated polymers for stretchable electronics applications.

1. Introduction

Polymer-based semiconductors are receiving more and more attention due to their intrinsic mechanical flexibility, solution processability and chemical tunability, together with their

applications in organic electronics like organic field effect transistors (OFET),[1–5] organic photovoltaics (OPV) and thermoelectrics.[6–11] Building upon the success of polythiophene polymers, recent efforts have been devoted to synthesizing new conjugated polymers such as low band-gap donor-acceptor (D-A) polymers to boost their charge carrier mobility for OFETs and power conversion efficiency (PCE) for OPVs.[12–18] Although great improvements have been achieved in devices' electronic and optical performance, there is an increasing need for improving their mechanical property, i.e., lower stiffness and higher stretchability,[19] laying a foundation for future applications in wearable, stretchable electronics,[20–22] and bioelectronics.[23,24]

Early studies on the mechanical property of conjugated polymers started from polythiophene polymers have shown that backbone engineering, side chain engineering, copolymerization with deformable blocks and physical blending can efficiently improve the stretchability and reduce the elastic modulus.[25–28] Similar methods were later applied to D-A polymers, a class of conjugated polymers with superior electrical performance relative to P3ATs.[20,29] Diketopyrrolopyrrole (DPP)-based conjugated polymers are one of heavily studied D-A semiconducting materials with a top performing charge mobility above 12 cm^2 V^{-1} s^{-1},[30–32] which is as good as the polycrystalline silicon, allowing many practical applications in electronic devices. Encouraged by its promising electronic property, several methods have been explored to improve the mechanical property of DPP-based polymers and unravel the role of backbone and side chain structure in their intrinsic stretchability and charge mobility in order to achieve the best of two worlds.[30,32–40]

Backbone engineering of the DPP polymer comes from two strategies, either by tuning conjugated donor or acceptor groups or flexible non-conjugated linker groups.[41–43] Along this line, Roth *et al*. investigated a library of low band-gap polymers and qualitatively concluded that fused rings on the backbone would increase the elastic modulus and reduce the ductility, while branched side chains will have an opposite effect.[41] Similar conclusions were drawn by

Lu *et al*., where DPP polymers with branched side chains were noticed to be less stiff and more stretchable than linear ones.[40,44] Lipomi and Mei *et al*. showed that by introducing flexible groups like alkyl chains to the conjugated backbone, the crack onset strain increased from 4% without spacer to 12% with 70% ratio of spacer while retaining a decent charge mobility around 0.05 cm$_2$ V$_{-1}$ s$_{-1}$.[42] Furthermore, carefully designed non-conjugated linkers can also improve the solution processability of DPP polymers, which can be dissolved in benign solvents.[45] Apart from backbone engineering, functional side chains were also used to improve the mechanical performance. Wang's work showed that covalent crosslinking between side chains using oligo-siloxane can improve the elasticity and the ductility of the system, while maintaining the electrical performance even after 500 cycles at 20% strain.[46] Non-covalent crosslinking like hydrogen bonding was also shown to be useful by introducing self-healable electrical and mechanical properties to the polymer system.[47,48] Despite the versatility in improving the mechanical performance of D-A polymers, the dynamics of the conjugated polymer backbone, described by the glass transition temperature, upon using isolated or fused thiophene linkers in the polymer backbone is still not well explored and hinders rational design of the conjugated polymers with target glass transition temperature as well as mechanical property.

Herein, we have systematically varied the main chain structure by inserting different donor moieties, including thiophene (T), bithiophene (T2), terthiophene (T3), thienothiophene (TT) and dithienothiophene (TTT) (**Figure 1a**) into the DPP polymer to study their impact on the thermomechanical property of conjugated polymer thin films. Our study revealed that all the thiophene building blocks act as anti-plasticizers and slow down the backbone dynamics, resulting in an increase in the elastic modulus for thin polymeric film. Further morphological studies on DPP thin films using grazing incidence wide-angle X-ray scattering (GIWAXS), atomic force microscopy (AFM) and ultraviolet visible spectroscopy (UV-Vis) showed that there is no significant influence of aggregation state on the mechanical property while the

degree of crystallinity would increase the elastic modulus slightly. Crystalline packing structure, degree of aggregation, and surface roughness do not directly correlate with the mechanical property of DPP polymers. This study provided new understanding of the effect of the thiophene unit insertion on the mechanical behaviors and chain dynamics of conjugated polymer thin films. Using the knowedge gained here, we finally designed and synthesized a new DPP polymer that has a record low backbone T_g and elastic modulus for the reported DPP family. This work will provide guidance to the future design of stretchable semiconducting polymers with desired thermomechanical property.

2. Results and Discussion

2.1. Thermomechanical property of DPP polymers

Five different DPP polymers were synthesized according to previous reports.[38,49–52] After the synthesis, the samples were purified and characterized by high temperature GPC in trichlorobenzene at 170 °C to gain insights into their molecular weight and polydispersity. **Figure 1a** and **Table 1** summarized the structure and the material's property of the synthesized DPP polymers.

We first probed the mechanical property of ~ 90 nm pseudo-free standing thin films using custom-made thin film tensile tester as shown in **Figure 1b**. The details of the set-up were described in our previous publication.[53] This methodology eliminates the effect of the supporting elastomeric substrates compared to another popular thin film mechanical characterization technique named "buckling metrology",[54] thus providing intrinsic mechanical property of the thin film. To provide a fair comparison between different DPP polymers, conjugated polymers with similar molecular weights were targeted and synthesized, followed by processing into thin films of similar thickness, and annealing at the same temperature. We carefully controlled the film thickness to be between 80 nm and 100 nm for all five samples by

changing the solution concentration, in order to avoid the influence of film thickness effect, also known as the confinement effect, on the mechanical property of thin films, as reported in previous studies.[53,55,56] The molecular weight is another factor that has been observed to critically influence the mechanical property of a given polymer, which was carefully tuned to be in the similar range, as shown in **Table 1**. The effect of film processing, film morphology, and molecular weight on their mechanical property will be discussed in more detail in the following section.

The representative stress-strain curves of DPP polymeric thin films with varying electron-donating units in the polymer backbone were shown in **Figure 1c** and **Figure 1d**. Each polymer was tested for more than six times and the average value of elastic modulus and crack onset strain were summarized in **Table 1**. We first discussed the influence of isolated thiophene units on the thin film mechanics, followed by the fused thiophene units. **Figure 1c** plotted the stress-strain curve of DPP-T, DPP-T2 and DPP-T3 (see **Figure 1**a for their chemical structure), which provided a close comparison for their mechanical behaviors. With the increasing number of isolated thiophene units on the backbone, the elastic modulus increased from 173 MPa for DPP-T to 281 MPa for DPP-T2, and 319 MPa for DPP-T3 for ~ 90 nm thin films. At first glance, the observation may seem contradictory since the incorporation of thiophene units into the backbone would be expected to increase the backbone flexibility. Donor-acceptor polymers typically have rigid polymer backbones and are less flexible. Here, we measured that DPP-T polymer has a persistence length of ~ 9 nm determined by small angle neutron scattering for dilute polymer in deuterated solvents (Figure S1). Previous report by Segalman group suggested that P3HT has more flexible, coiled chain with persistence length of ~3 nm.[57] Thus inserting more thiophene units would likely to reduce backbone rigidity. This interesting observation of increased elastic modulus upon incorporating thiophene units was later rationalized by the T_g of DPP polymers. The observed increase in elastic modulus is closely correlated with the

increased T_g measured in both thin film and bulk state of conjugated polymers (discussed in more detail in the later part). On the other hand, the stretchability, using crack onset strain as metric, showed less significant difference among three DPP polymers with different amounts of isolated thiophene units. Free-standing DPP-T thin films on average can be impressively stretched up to 53% of strain while the other two DPP polymers reached 44% of strain before the formation of cracks. Both crack onset strain reached record-high value compared to other pseudo free standing test results reported previously for pure donor-acceptor polymeric thin films (see Table S4 in the Supporting Information for a summary of previous reported values). We attribute this observation to the high molecular weight for these three DPP polymers synthesized here, as well as below room temperature backbone T_g.

In addition to tensile pulling test, stress-relaxation test provided insights into the viscoelastic property of the conjugated polymer, thus was performed on DPP-T, DPP-T2 and DPP-T3 polymers. The polymer film was stretched to 2% strain at the strain rate of $1*10_{-3}$ s$_{-1}$ then measured the stress relaxation. The stress was recorded as a function of time and plotted in **Figure 1e**. The Kohlrausch-Williams-Watts (KWW) equation was used to obtain the relaxation time for molecular chains to gain insights into the chain dynamics.[58] Detailed fitting information can be found in Figure S2 of the Supporting Information. The average relaxation time was 116 s, 3563 s, 6058 s for DPP-T, DPP-T2, DPP-T3, respectively. This is in good agreement with the observed trend for T_g, and further supported that the insertion of the thiophene unit will slow the backbone dynamics.

For DPP polymers with fused thiophene rings on the backbone, the increase in elastic modulus was more distinct, from 173 MPa for DPP-T to 480 MPa for DPP-TTT, as shown in **Figure 1d**. In the meantime, the decay in crack onset strain was substantial with increased size of fused rings, from 53% to 3%. This phenomenon agreed well with previous research demonstrating

that polymers with fused rings have higher stiffness and higher tendency to break upon tensile strain than polymers with isolated rings.[41]

The molecular weight of the conjugated polymer can greatly influence a given polymer's mechanical property.[59,60] Consequently, we also studied thin film mechanical property for three DPP polymers (DPP-T, DPP-T2, and DPP-TT) with a lower molecular weight (M_n = ~ 25 kDa), as opposed to DPP polymers with M_n around 50 kDa as shown in **Figure 1**. We found little difference in the value of the elastic modulus on molecular weight, while higher M_n consistently leads to higher crack onset strain, which can be attributed to increased inter-chain entanglements between DPP chains (Figure S3, Supporting Information).[60,61] Surpassing the entanglement molecular weight of a given conjugated polymer is important to enhance its crack onset strain. Although we were not able to measure the critical entanglement molecular weight for DPP conjugated polymers, the mechanical tensile test suggested that critical entanglement molecular weight is likely to be below 50 kDa, thus significant intermolecular chain entanglements resulted in good deformability of these three samples reported in **Figure 1**.

The effect of thermal treatment on the mechanical property was also investigated. Figure S4 showed the stress-strain curves for DPP-T, DPP-T2 and DPP-TT polymers before and after thermal annealing at 200 °C for 10 mins (Supporting Information). The elastic modulus increased slightly by ~ 10% while the stretchability decreased by ~ 20%, due to increased degree of crystallinity upon annealing. The detailed analysis on the thin film morphology will be discussed in the following section.

To rationalize the change in elastic modulus upon insertion of thiophene building blocks, we measured the T_g for five DPP polymers in both bulk state by using DMA and in thin film state by AC chip calorimetry. Previous work indicated the challenge of using DSC to probe weak transitions for conjugated polymers.[62] Thus, we used two techniques that are sensitive to the

T_g, and the results were summarized in **Table 1**. **Figure 2** showed the results for DMA analysis including the T_g of five DPP polymers. Here, we identified the major peak on the tan δ curve as the backbone T_g. We assigned relative weak shoulders around -50 °C to be the T_g of the flexible alkyl side chain, which can be observed in all five polymers. The side chain transition peak was more pronounced as observed in the loss modulus curve. Only the side chain T_g can be measured by DSC (Figure S5, Supporting Information), which agreed with previously reported literature.[40] From **Figure 2a** to **2c**, we observed a noticeable increase of backbone T_g from -3.96 °C (DPP-T) to 11.95 °C (DPP-T2), and 18.98 °C (DPP-T3) as the number of thiophene units increased (**Table 1**). Similarly, when comparing **Figure 2a**, **2d** and **2e**, the T_g increased from -3.96 °C (DPP-T) to 2.76°C (DPP-TT), and 4.11 °C (DPP-TTT) as the size of fused ring structure enlarged. The increase in T_g synchronized with the observed increase in elastic modulus. We further used AC-chip calorimetry to characterize the conjugated polymer's T_g in the thin film state. The exact value of T_g is not the same since the glass transition is a kinetic property and highly depends on probing techniques and measurement conditions (e.g. cooling or heating rate). However, the same trend in the probed T_g values was observed using the AC-chip calorimetry (Figure S6, Supporting Information). Additionally, we also investigated the molecular weight effect on T_g. DPP polymers with low molecular weight (~ 25 kDa) were tested. The difference in T_g was insignificant with only 3 °C difference being observed (Figure S7, Supporting Information), which explained the similar elastic modulus between different molecular weights of polymers observed above. The weak dependence of T_g on molecular weight can be rationalized by the Flory-Fox equation, which predicted the weak dependence of T_g on the molecular weight at high molecular weight region.[63,64] Both bulk and thin film techniques suggested the incorporation of the electronic donating group into the polymer structure greatly altered its backbone dynamics, and reflected in their macroscopic mechanical properties.

9

Although the focus of this paper is not on the electronic property of conjugated polymers, we measured the charge carrier mobility of five samples using thin film transistors with doped silicon as bottom gate electrode, silicon dioxide as the dielectric layer and evaporated gold as source and drain electrode. We found that all the five polymers showed decent electronic property, ranging from $0.03 \sim 1$ cm$_2$ V$_{-1}$ s$_{-1}$ (Table S1). The transfer curve for all the measurements were provided in Figure S8 of the Supporting Information. We also summarized the charge carrier mobility data for previously reported DPP polymers with thiophene units as the donor unit in Table S5. Due to the difference in the molecular weight and processing method, our reported mobility data was not the highest among reported works.

2.2 The relationship between mechanical property and morphology

We used multiple morphology characterization techniques, including GIWAXS, UV-Vis and AFM, to understand the potential correlation between the morphology and mechanical property for the DPP polymers. Firstly, the degree of crystallinity and molecular packing lattice parameter in the crystalline region of five DPP thin films were measured by GIWAXS, before and after thermal annealing. All DPP polymers exhibited semicrystalline structures. The 2D scattering patterns and the 1D line-cut profiles (both in plane and out of plane scattering profile) were shown in **Figure 3** for annealed films and Figure S9 for as-deposited films in the Supporting Information, respectively. For as-cast polymers, a bimodal orientation, both edge-on and face-on orientation, was shown, as evidenced by (010) π-π stacking peak presented in both in plane and out of plane direction. DPP-T exhibited mostly face-on orientation and less ordered crystalline domain, as inferred from the large full width at half maximum (FWHM) for (100) peak and the absence of high-order diffraction peaks. In contrast, other polymers showed a preference for edge-on orientation and high-order (h00) peaks. Upon annealing, the fraction of edge-on orientation increased for all polymers, evidenced by much weaker (010) peak along the q$_z$ axis and stronger (010) peak along the q$_{xy}$ axis. Also, improved microstructural ordering

10

was shown, judging from the more intense elliptical shape of (h00) peaks. These observations are similar to previous reports from Zhang *et al.* for DPP-T, DPP-T2 and DPP-TT polymers.[65] The key parameters of chain packing for conjugated polymers were summarized in **Table 2**. In this study, the π-π stacking distance showed no obvious trend concerning varied backbone structures, while DPP-TTT has the closest packing distance of 3.59 Å among the five polymers, which could arise from its greater coplanarity due to its large fused ring. On the contrary, the lamellar packing distance showed a clear trend upon systematically varying the main chain structure. With more isolated thiophene units incorporated into the DPP backbone, the d-spacing distance gradually dropped from 23.44 Å for DPP-T to 22.20 Å for DPP-T2, and 20.67 Å for DPP-T3 in annealed samples. Similarly, as the size of fused thiophene rings increases, the lamellar packing distance decreased to 22.60 Å for DPP-TT, and 21.67 Å for DPP-TTT. This is because side chains attached to the DPP moiety can fold into the extra space created by less bulky thiophene units between DPP building blocks (Scheme S2, Supporting Information). Similar observation was reported previously in other conjugated polymer systems.[66,67] The FWHM for the (100) peak increased with the number of thiophene units or the size of fused thiophene rings, which indicated a reduction in the polymer crystallite size. To further quantify the effect of film morphology on mechanical properties, we extracted the relative degree of crystallinity (RDoC) for annealed polymers and plotted in **Figure 3**, detailed procedures to obtain RDoC can be found in Figure S10 (Supporting Information) as well as previous reports by Baker *et al.*[68–70] Judged from the (100) pole figures, the relative degree of crystallinity increased in the order of DPP-T < DPP-T2 < DPP-T3, and DPP-T < DPP-TT < DPP-TTT, which is consistent with the trend of elastic modulus. Despite similar RDoC between DPP-T2 and DPP-TT, or between DPP-T3 and DPP-TTT, there is still 50% difference in elastic modulus between two polymers, which could be mostly attributed to the different T_g and backbone rigidity between two polymers. Thus the RDoC played a secondary role in influencing the mechanical property of the conjugated polymer film, after the glass transition temperature.

AFM was performed on both as cast (Figure S11, Supporting Information) and thermally annealed polymer films (**Figure 4**) to study the film morphology using tapping mode. All five samples displayed similar nanofibrillar textures. The film roughness (Ra) for all films was within 1 nm, which can be attributed to their good solubility in chlorobenzene solvent. There is no direct correlation between the mechanical property with surface morphology of conjugated polymers. The UV-Vis absorption spectra were measured in thin film state (Figure S12, Supporting Information). It is noted that two absorption bands were presented, corresponding to the π-π* transition (400 to 460 nm) and intramolecular coupling between donor and acceptor units (700 to 850 nm), which is consistent with previous studies on DPP-based conjugated polymers.[40,48] The aggregation behavior was investigated by comparing the relative intensity of peak 0-1 and peak 0-0, the result indicated slight difference in the aggregation behavior for the polymer chain, e.g., DPP-T3 showed 11% decrease in short-range aggregation when compared with DPP-T. The absorption peak positions and peak areas were summarized in Table S2 and Table S3 of the Supporting Information, respectively. We did not observe clear correlation between the aggregation state of the DPP polymer films with respective to their mechanical property.

Through the detailed morphological characterization, we found that the crystallinity could increase the fraction of hard-rigid phase in the thin films thus increase their elastic modulus slightly. The degree of order in the amorphous aggregation phase did not influence the apparent elastic modulus which can be attributed to the fact that the probed aggregation order is in the short range (e.g. inter π-π interaction).

2.3 Influence of the side chain on the backbone T_g

From our experimental results, we found that adding either isolated or fused thiophene rings in the backbone both raised the backbone T_g and consequently the elastic modulus of the

polymeric thin film. The glass transition temperature of the DPP polymer upon addition of thiophene building blocks can be estimated by classic Fox equation (Equation 1).[71]

$$\frac{1}{T_g} = \frac{w_1}{T_{g,1}} + \frac{w_2}{T_{g,2}}$$ (1)

Since DPP polymers can be viewed as the DPP unit and the inserted donor unit, the T_g can be treated to be the combinatory effect of two individual components. For example, the T_g of DPP-T is -3.96 °C, and the T_g of a polythiophene polymer without side chain was previously determined to be around 120 °C.[72] Upon incorporating one additional thiophene unit, the T_g of DPP-T2 can be calculated to be around 3 °C, and 13 °C for DPP-T3 using Equation 1. The calculated result agrees well with experimentally measured T_g for DPP-T2 and DPP-T3. For DPP polymers with fused thiophene rings, we were not able to perform similar calculation since there is no reported T_g of fused thiophene rings.

Besides DPP-based polymer system, the above trend was also observed in the quinoidal *para*-azaquinodimethane (*p*-AQM)-based low-bandgap conjugated polymers.[67] As shown in **Figure 5**, the T_g of two polymers (PA3T-BC2-C10C12 and PA4T-BC2-C10C12) with increased number of backbone thiophene units were compared. With one additional thiophene unit inserted into the polymer backbone while maintaining the same side chain length, PA4T-BC2-C10C12 showed 25 °C increase in T_g than that of PA3T-BC2-C10C12. This observation indicated that the anti-plasticization effect upon inserting thiophene units to the backbone can be a general phenomenon for conjugated polymers.

2.4 Engineering low T_g and low modulus DPP polymers

Encouraged by our findings above, we aim to go to the opposite direction by incorporating the low T_g component into the DPP system to reduce its T_g. Another DPP-based polymer was purposely designed and synthesized by incorporating DPP unit with an alkyl chain decorated

thiophene unit. The chemical structure and mechanical property of this new polymer (DPP-T3-C8) were shown in **Figure 6**. Detailed synthesis of this polymer can be found in the Supporting Information. The number average molecular weight of the new DPP polymer is 26.8 kDa, with a polydispersity of 2.5. Through additional side chains on the thiophene unit, we effectively increased the weight fraction of the side chain to 64.9%. Consequently, the T_g of DPP-T3-C8 polymer dropped from 18.98 °C for reference polymer DPP-T3 to -11.83 °C. Using this strategy, we were able to reach a record low elastic modulus for DPP polymers down to 150 MPa. Compared to DPP-T3 with a similar molecular weight, the crack onset strain was decreased from 44 % to 35%, representing a 20% decrease.

We further surveyed the previously reported work on the DPP polymers with various side chain lengths and listed them in Table S5 of the Supporting Information. There are several popular side chain length choices, 2-hexyloctyl (2-HO), 2-octyldodecyl (2-OD), and 2-decyl dodecyl (2-DD). Those DPP polymers have sixteen carbons, twenty carbons, and twenty-four carbons in the polymer side chain respectively. Using volume fraction of side chain as a measurement metric, the DPP-T3 polymer with three different side chain lengths would have varied weight fractions of the side chain of 55.0% (2-HO), 57.1% (2-OD) and 58.9% (2-DD), respectively. Previously reported DPP-TT polymer, for example, is mostly focused on the 2-octyldodecyl (2-OD) side chains, thus would result in lower side chain content, high T_g, higher elastic modulus and lower crack onset strain. A systematic study of the side chain length is outside the scope of this work and will be reported in a separate work.

3. Conclusion

In summary, this paper studied the effect of thiophene based electron-rich building block on the thermomechanical property and morphology of semiconducting polymers. Five different DPP-based polymers with isolated thiophene units (DPP-T, DPP-T2, DPP-T3) and fused thiophene rings (DPP-TT, DPP-TTT) were systematically synthesized, their thermomechanical properties

were measured and compared. The addition of thiophene units or fused thiophene rings resulted in the increase in the T_g of the polymer measured in both bulk and thin film state and appeared as an increase in its elastic modulus. These behaviors can be related to the addition of high-T_g chemical moieties to the main chain, i.e., reduction in low temperature side chain fraction. This observation can be generally applied to other conjugated polymer systems. Based on the results above, we engineered a new stretchable DPP-based polymer DPP-T3-C8 by increasing the side chain content on the thiophene unit. With the elastic modulus as low as 150 MPa, and T_g of -11.8 °C, the polymer showed 50% decrease in elastic modulus and 35% in stretchability. Taken together, this study demonstrated that controlling low-T_g side chain content is an efficient way to develop new stretchable conjugated polymers.

4. Experimental Section

Materials and processing: Five DPP-based conjugated polymers with systematically controlled main chain structures were synthesized. The electron donating unit was varied by introducing different numbers of thiophene units or sizes of fused thiophene rings. Their chemical structures were shown in **Figure 1a**. The synthesis procedures of DPP-T,[65,73] DPP-T2,[50,51] DPP-T3,[38] DPP-TT[49,74] and DPP-TTT[52] have been reported elsewhere. The number molecular weight was measured by high temperature gel permeation chromatography (HT-GPC) using trichlorobenzene as the eluent at 160 °C, polystyrene for calibration, viscometer and light scattering as the detector. One additional purposely engineered DPP-based conjugated polymer with additional flexible alkyl chains on the thiophene unit (Scheme S1) has been synthesized using a protocol detailed in Supporting Information. Polymer thin films were fabricated by spin coating of conjugated polymer solutions in chlorobenzene (CB) on the silicon substrate with native oxide layer. Thermal annealing of the deposited polymer film was performed at 200 °C for 10 mins inside of a glove box and allowed to cool down to room temperature before additional testing.

Small angle neutron scattering: Small-angle neutron scattering (SANS) study was performed at the extended Q-range small-angle neutron scattering diffractometer (EQ-SANS BL-6) line at the Spallation Neutron Source (SNS) located at Oak Ridge National Laboratory (ORNL). Two wavelengths and their corresponding sample-to-detector distances were used to obtain a wide q range: 2.5 Å at 2.5 m, and 8 Å at 8 m. The solution was made by dissolving the polymer in deuterated chlorobenzene with a concentration of 5 mg/ml. Data reduction was performed in MantidPlot to obtain the polymer scattering data by subtracting the solution signal with solvent scattering signal. Later, the obtained polymer scattering data was fitted by using SasView.

Pseudo-free Standing Tensile Test: Thin film tensile tests were performed on the water surface through pseudo-free-standing tensile tester. Details about the tensile stage setup can be referred to our previous publication.[53] Briefly speaking, the polymer thin films (~ 90 nm) were patterned into dog-bone shape by oxygen plasma etching process and floated on top of water before being further unidirectionally pulled at a strain rate of $5*10^{-4}$ s^{-1} until the film fractures. At least six independent samples were measured for each conjugated polymer to provide statistically averaged mechanical property. The elastic modulus was obtained from the slope of the linear fit of the stress-strain curve using the first 0.5% strain (elastic region).

Dynamic Mechanical Analysis (DMA): DMA measurements were performed on a TA Q800 DMA.[75] Samples were prepared by drop casting of polymer solutions on top of glass fibers. In this test, the backbone T_g was determined to be the peak temperature corresponding to the peak of tan δ for all samples.

Alternating Current (AC) Chip Calorimetry: The AC chip calorimeter was used to obtain the glass transition temperature of the polymeric thin film.[76] The experiments were performed at a frequency of 10 Hz and a heating/cooling rate of 1 °C/min. The dynamic glass transition

temperature was determined as the half-step temperature of the amplitude of the complex differential voltage.

Grazing Incidence Wide Angle X-ray Scattering (GIWAXS): GIWAXS experiments were performed on beamline 11-3 at the Stanford Synchrotron Radiation Lightsource (SSRL). Data was collected under helium environment with an incident beam energy at 12.7 keV and an incidence angle of 0.12°. The sample to detector distance is about 300 mm. Diffraction data analysis was performed using Nika software package for Wavemetrics Igor, in combination with WAXStools.

Atomic Force Microscopy (AFM): AFM images were acquired on Bruker Dimension Icon in tapping mode. The samples were casted on the flat silicon substrate as described above.

UV-Vis-NIR Absorption Spectroscopy: The solid-state UV-Vis-NIR spectra were recorded on Agilent Cary 5000 using polymer thin films deposited on glass slides.

Supporting Information
Supporting Information is available from the Wiley Online Library or from the author.

References

[1] H. Sirringhaus, *Adv. Mater.* **2014**, *26*, 1319.

[2] C. Wang, H. Dong, W. Hu, Y. Liu, D. Zhu, *Chem. Rev.* **2012**, *112*, 2208.

[3] V. Podzorov, *MRS Bull.* **2013**, *38*, 15.

[4] H. Dong, X. Fu, J. Liu, Z. Wang, W. Hu, *Adv. Mater.* **2013**, *25*, 6158.

[5] A. F. Paterson, S. Singh, K. J. Fallon, T. Hodsden, Y. Han, B. C. Schroeder, H. Bronstein, M. Heeney, I. Mcculloch, T. D. Anthopoulos, *Adv. Mater.* **2018**, 1801079.

[6] L. Lu, T. Zheng, Q. Wu, A. M. Schneider, D. Zhao, L. Yu, *Chem. Rev.* **2015**, *115*, 12666.

[7] Y. Li, W. K. Tatum, J. W. Onorato, S. D. Barajas, Y. Y. Yang, C. K. Luscombe, *Polym. Chem.* **2017**, *8*, 5185.

[8] G. Li, R. Zhu, Y. Yang, *Nat. Photonics* **2012**, *6*, 153.

[9] R. A. J. Janssen, J. Nelson, *Adv. Mater.* **2013**, *25*, 1847.

[10] A. J. Heeger, *Adv. Mater.* **2014**, *26*, 10.

[11] B. Russ, A. Glaudell, J. J. Urban, M. L. Chabinyc, R. A. Segalman, *Nat. Rev. Mater.* **2016**, *1*, 16050.

[12] K. Müllen, W. Pisula, *J. Am. Chem. Soc.* **2015**, *137*, 9503.

[13] V. Coropceanu, J. Cornil, D. Silva, D. A, Y. Olivier, R. Silbey, J. L. Bredas, D. A. da Silva Filho, J.-L. J.-L. Brédas, Y. Olivier, R. Silbey, J.-L. J.-L. Brédas, *Chem. Rev.* **2007**, *107*, 926.

[14] A. T. Kleinschmidt, S. E. Root, D. J. Lipomi, *J. Mater. Chem. A* **2017**, *5*, 11396.

[15] J. Hou, O. Inganas, R. H. Friend, F. Gao, *Nat. Mater.* **2018**, *17*, 119.

[16] S. Zhang, Y. Qin, J. Zhu, J. Hou, *Adv. Mater.* **2018**, 1800868.

[17] J. Zhang, B. Kan, A. J. Pearson, A. J. Parnell, J. F. K. Cooper, X. K. Liu, P. J. Conaghan, T. R. Hopper, Y. Wu, X. Wan, F. Gao, N. C. Greenham, A. A. Bakulin, Y. Chen, R. H. Friend, *J. Mater. Chem. A* **2018**, *6*, 18225.

[18]   L. Meng, Y. Zhang, X. Wan, C. Li, X. Zhang, Y. Wang, X. Ke, Z. Xiao, L. Ding, R. Xia, H. L. Yip, Y. Cao, Y. Chen, *Science.* **2018**, *361*, 1094.

[19]   S. Savagatrup, A. D. Printz, D. Rodriquez, D. J. Lipomi, *Macromolecules* **2014**, *47*, 1981.

[20]   M. U. Ocheje, B. P. Charron, A. Nyayachavadi, S. Rondeau-Gagné, *Flex. Print. Electron.* **2017**, *2*, 043002.

[21]   G. J. N. Wang, A. Gasperini, Z. Bao, *Adv. Electron. Mater.* **2018**, *4*, 1700429.

[22]   S. E. Root, S. Savagatrup, A. D. Printz, D. Rodriquez, D. J. Lipomi, *Chem. Rev.* **2017**, *117*, 6467.

[23]   A. Chortos, J. Liu, Z. Bao, *Nat. Mater.* **2016**, *15*, 937.

[24]   T. Someya, Z. Bao, G. G. Malliaras, *Nature* **2016**, *540*, 379.

[25]   B. O'Connor, E. P. Chan, C. Chan, B. R. Conrad, L. J. Richter, R. J. Kline, M. Heeney, I. McCulloch, C. L. Soles, D. M. DeLongchamp, *ACS Nano* **2010**, *4*, 7538.

[26]   C. Müller, S. Goffri, D. W. Breiby, J. W. Andreasen, H. D. Chanzy, R. A. J. Janssen, M. M. Nielsen, C. P. Radano, H. Sirringhaus, P. Smith, N. Stingelin-Stutzmann, *Adv. Funct. Mater.* **2007**, *17*, 2674.

[27]   M. Chang, D. Choi, G. Wang, N. Kleinhenz, N. Persson, B. Park, E. Reichmanis, *ACS Appl. Mater. Interfaces* **2015**, *7*, 14095.

[28]   D. Choi, H. Kim, N. Persson, P. H. Chu, M. Chang, J. H. Kang, S. Graham, E. Reichmanis, *Chem. Mater.* **2016**, *28*, 1196.

[29]   S. Holliday, J. E. Donaghey, I. McCulloch, *Chem. Mater.* **2014**, *26*, 647.

[30]   I. Kang, H. J. Yun, D. S. Chung, S. K. Kwon, Y. H. Kim, *J. Am. Chem. Soc.* **2013**, *135*, 14896.

[31]   J. T. E. Quinn, J. Zhu, X. Li, J. Wang, Y. Li, *J. Mater. Chem. C* **2017**, *5*, 8654.

[32]   C. B. Nielsen, M. Turbiez, I. McCulloch, *Adv. Mater.* **2013**, *25*, 1859.

[33]   G. J. N. Wang, A. Gasperini, Z. Bao, *Adv. Electron. Mater.* **2018**, *4*, 1700429.

[34] J. Xu, S. Wang, G. J. N. Wang, C. Zhu, S. Luo, L. Jin, X. Gu, S. Chen, V. R. Feig, J. W. F. To, S. Rondeau-Gagné, J. Park, B. C. Schroeder, C. Lu, J. Y. Oh, Y. Wang, Y. H. Kim, H. Yan, R. Sinclair, D. Zhou, G. Xue, B. Murmann, C. Linder, W. Cai, J. B. H. Tok, J. W. Chung, Z. Bao, *Science.* **2017**, *355*, 59.

[35] D. J. Lipomi, Z. Bao, *Energy Environ. Sci.* **2011**, *4*, 3314.

[36] H. C. Wu, S. J. Benight, A. Chortos, W. Y. Lee, J. Mei, J. W. F. To, C. Lu, M. He, J. B. H. Tok, W. C. Chen, Z. Bao, *Chem. Mater.* **2014**, *26*, 4544.

[37] Y. Zhao, X. Zhao, Y. Zang, C. A. Di, Y. Diao, J. Mei, *Macromolecules* **2015**, *48*, 2048.

[38] Z. Yi, X. Sun, Y. Zhao, Y. Guo, X. Chen, J. Qin, G. Yu, Y. Liu, *Chem. Mater.* **2012**, *24*, 4350.

[39] H. S. Kim, E. Song, S. B. Lee, I. N. Kang, K. Cho, D. H. Hwang, *Org. Electron. physics, Mater. Appl.* **2018**, *56*, 129.

[40] B. C. Schroeder, T. Kurosawa, T. Fu, Y. C. Chiu, J. Mun, G. J. N. Wang, X. Gu, L. Shaw, J. W. E. Kneller, T. Kreouzis, M. F. Toney, Z. Bao, *Adv. Funct. Mater.* **2017**, 1701973.

[41] B. Roth, S. Savagatrup, N. V. De Los Santos, O. Hagemann, J. E. Carlé, M. Helgesen, F. Livi, E. Bundgaard, R. R. Søndergaard, F. C. Krebs, D. J. Lipomi, *Chem. Mater.* **2016**, *28*, 2363.

[42] S. Savagatrup, X. Zhao, E. Chan, J. Mei, D. J. Lipomi, *Macromol. Rapid Commun.* **2016**, *37*, 1623.

[43] B. C. Schroeder, Y. C. Chiu, X. Gu, Y. Zhou, J. Xu, J. Lopez, C. Lu, M. F. Toney, Z. Bao, *Adv. Electron. Mater.* **2016**, *2*, 1600104.

[44] C. Lu, W. Y. Lee, X. Gu, J. Xu, H. H. Chou, H. Yan, Y. C. Chiu, M. He, J. R. Matthews, W. Niu, J. B. H. Tok, M. F. Toney, W. C. Chen, Z. Bao, *Adv. Electron. Mater.* **2017**, *3*, 1600311.

[45]   G. N. Wang, F. Molina-lopez, H. Zhang, J. Xu, H. Wu, L. Shaw, J. Mun, Q. Zhang, S. Wang, A. Ehrlich, Z. Bao, *Macrolmolecules* **2018**, *51*, 4976.

[46]   G. J. N. Wang, L. Shaw, J. Xu, T. Kurosawa, B. C. Schroeder, J. Y. Oh, S. J. Benight, Z. Bao, *Adv. Funct. Mater.* **2016**, *26*, 7254.

[47]   J. Y. Oh, S. Rondeau-Gagné, Y. C. Chiu, A. Chortos, F. Lissel, G. J. N. Wang, B. C. Schroeder, T. Kurosawa, J. Lopez, T. Katsumata, J. Xu, C. Zhu, X. Gu, W. G. Bae, Y. Kim, L. Jin, J. W. Chung, J. B. H. Tok, Z. Bao, *Nature* **2016**, *539*, 411.

[48]   M. U. Ocheje, B. P. Charron, Y. H. Cheng, C. H. Chuang, A. Soldera, Y. C. Chiu, S. Rondeau-Gagné, *Macromolecules* **2018**, *51*, 1336.

[49]   J. C. Bijleveld, R. A. M. Verstrijden, M. M. Wienk, R. A. J. Janssen, *J. Mater. Chem.* **2011**, *21*, 9224.

[50]   J. S. Ha, K. H. Kim, D. H. Choi, *J. Am. Chem. Soc.* **2011**, *133*, 10364.

[51]   Y. Li, P. Sonar, L. Murphy, W. Hong, *Energy Environ. Sci.* **2013**, *6*, 1684.

[52]   J. W. Jung, F. Liu, T. P. Russell, W. H. Jo, *Energy Environ. Sci.* **2012**, *5*, 6857.

[53]   S. Zhang, M. U. Ocheje, S. Luo, B. Appleby, D. Weller, S. Rondeau-gagné, X. Gu, *Macromol. Rapid Commun.* **2018**, 1800092.

[54]   C. M. Stafford, C. Harrison, K. L. Beers, A. Karim, E. J. Amis, M. R. Vanlandingham, H. C. Kim, W. Volksen, R. D. Miller, E. E. Simonyi, *Nat. Mater.* **2004**, *3*, 545.

[55]   Y. Liu, Y. C. Chen, S. Hutchens, J. Lawrence, T. Emrick, A. J. Crosby, *Macromolecules* **2015**, *48*, 6534.

[56]   L. Si, M. V. Massa, K. Dalnoki-Veress, H. R. Brown, R. A. L. Jones, *Phys. Rev. Lett.* **2005**, *94*, 127801.

[57]   B. McCulloch, V. Ho, M. Hoarfrost, C. Stanley, C. Do, W. T. Heller, R. A. Segalman, *Macromolecules* **2013**, *46*, 1899.

[58]   C. Watts, E. Davies, *Trans. Faraday Soc.* **1969**, *66*, 80.

[59] F. P. V. Koch, J. Rivnay, S. Foster, C. Müller, J. M. Downing, E. Buchaca-Domingo, P. Westacott, L. Yu, M. Yuan, M. Baklar, Z. Fei, C. Luscombe, M. A. McLachlan, M. Heeney, G. Rumbles, C. Silva, A. Salleo, J. Nelson, P. Smith, N. Stingelin, *Prog. Polym. Sci.* **2013**, *38*, 1978.

[60] D. Rodriquez, J.-H. Kim, S. E. Root, Z. Fei, P. Boufflet, M. Heeney, T.-S. Kim, D. J. Lipomi, *ACS Appl. Mater. Interfaces* **2017**, *9*, 8855.

[61] C. Bruner, R. Dauskardt, *Macromolecules* **2014**, *47*, 1117.

[62] G. Xue, X. Zhao, G. Qu, T. Xu, A. Gumyusenge, Z. Zhang, Y. Zhao, Y. Diao, H. Li, J. Mei, *ACS Appl. Mater. Interfaces* **2017**, *9*, 25426.

[63] T. G. Fox, P. J. Flory, *J. Appl. Phys.* **1950**, *21*, 581.

[64] R. Xie, Y. Lee, M. P. Aplan, N. J. Caggiano, C. Müller, R. H. Colby, E. D. Gomez, *Macromolecules* **2017**, *50*, 5146.

[65] X. Zhang, L. J. Richter, D. M. Delongchamp, R. J. Kline, M. R. Hammond, I. McCulloch, M. Heeney, R. S. Ashraf, J. N. Smith, T. D. Anthopoulos, B. Schroeder, Y. H. Geerts, D. A. Fischer, M. F. Toney, *J. Am. Chem. Soc.* **2011**, *133*, 15073.

[66] J. S. Lee, S. K. Son, S. Song, H. Kim, D. R. Lee, K. Kim, M. J. Ko, D. H. Choi, B. S. Kim, J. H. Cho, *Chem. Mater.* **2012**, *24*, 1316.

[67] X. Liu, B. He, A. Garzón-ruiz, A. Navarro, T. L. Chen, M. A. Kolaczkowski, S. Feng, L. Zhang, C. A. Anderson, *Adv. Funct. Mater.* **2018**, 1801874.

[68] Y. Diao, Y. Zhou, T. Kurosawa, L. Shaw, C. Wang, S. Park, Y. Guo, J. A. Reinspach, K. Gu, X. Gu, B. C. K. Tee, C. Pang, H. Yan, D. Zhao, M. F. Toney, S. C. B. Mannsfeld, Z. Bao, *Nat. Commun.* **2015**, *6*, 7955.

[69] J. Rivnay, S. C. B. Mannsfeld, C. E. Miller, A. Salleo, M. F. Toney, *Chem. Rev.* **2012**, *112*, 5488.

[70] J. L. Baker, L. H. Jimison, S. Mannsfeld, S. Volkman, S. Yin, V. Subramanian, A. Salleo, A. P. Alivisatos, M. F. Toney, *Langmuir* **2010**, *26*, 9146.

[71] T. Sasaki, A. Shimizu, T. H. Mourey, C. T. Thurau, M. D. Ediger, *J. Chem. Phys.* **2003**, *119*, 8730.

[72] S. A. Chen, J. M. Ni, *Macromolecules* **1992**, *25*, 6081.

[73] R. A. J. J. Johan C. Bijleveld, Arjan P. Zoombelt, Simon G. J. Mathijssen, Martijn M. Wienk, Mathieu Turbiez, Dago M. de Leeuw, *J. Am. Chem. Soc.* **2009**, *131*, 16616.

[74] G. Zhang, Y. Fu, Z. Xie, Q. Zhang, *Sol. Energy Mater. Sol. Cells* **2011**, *95*, 1168.

[75] A. Sharma, X. Pan, J. A. Campbell, M. R. Andersson, D. A. Lewis, *Macromolecules* **2017**, *50*, 3347.

[76] D. Zhou, H. Huth, Y. Gao, G. Xue, C. Schick, *Macrolmolecules* **2008**, *41*, 7662.
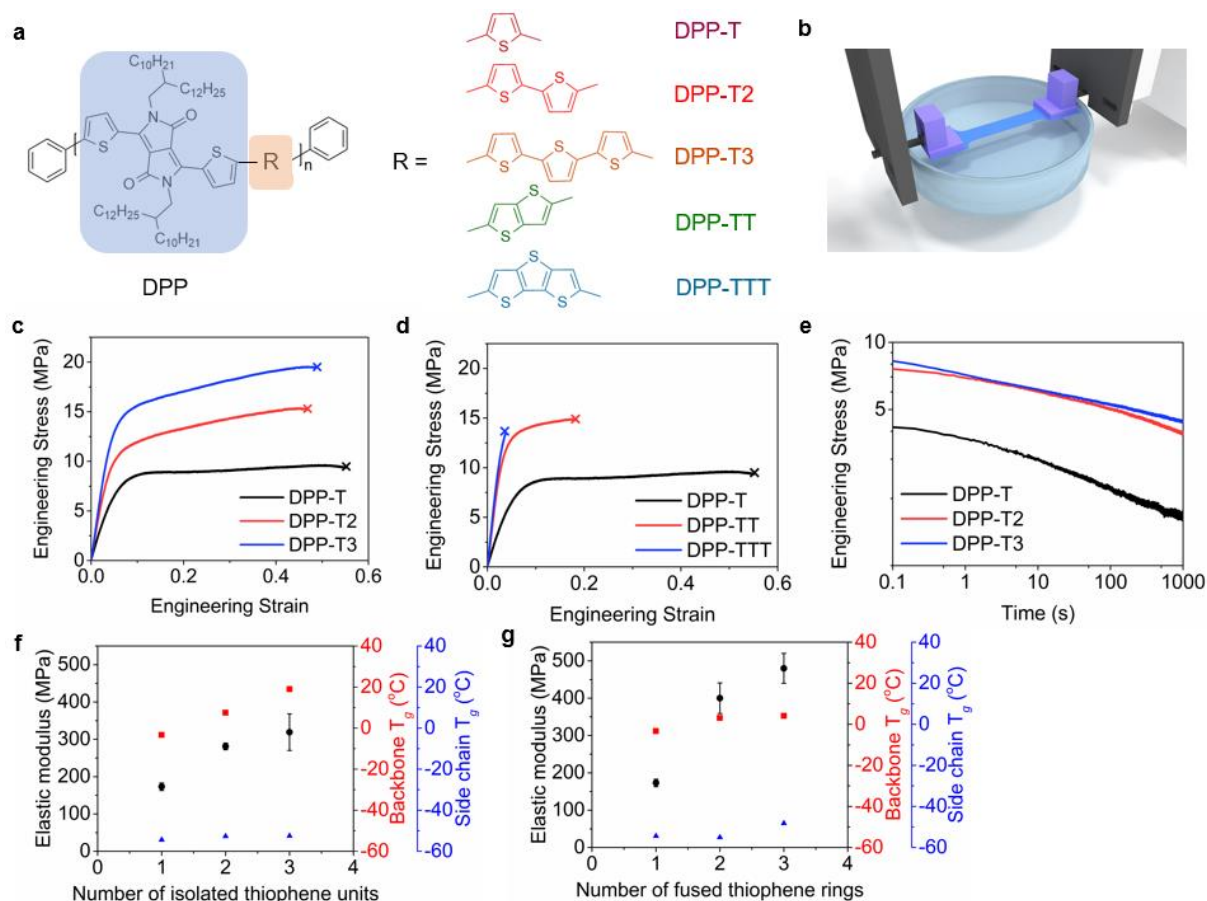
Figure 1. Thin film mechanical property of various DPP polymers. (a) Chemical structures of DPP polymers with different number of isolated thiophene units and fused thiophene rings. (b) Scheme of pseudo-free standing tensile test set-up. Comparison of stress strain curves for as-cast DPP-based D-A polymer ($M_n \sim 50$ kDa) films around 90 nm thick. (c) Stress strain curves for thin DPP polymer films with different numbers of thiophene units, DPP-T, DPP-T2 and DPP-T3; and (d) different sizes of fused thiophene rings, DPP-T, DPP-TT and DPP-TTT. (e) Stress-relaxation behaviors of DPP-T, DPP-T2 and DPP-T3. The data is in double logarithmic scale. The speed of decaying represents the speed of relaxation of polymer chain at room temperature. The elastic modulus, backbone and side chain glass transition temperature of DPP polymers are shown in (f) and (g).
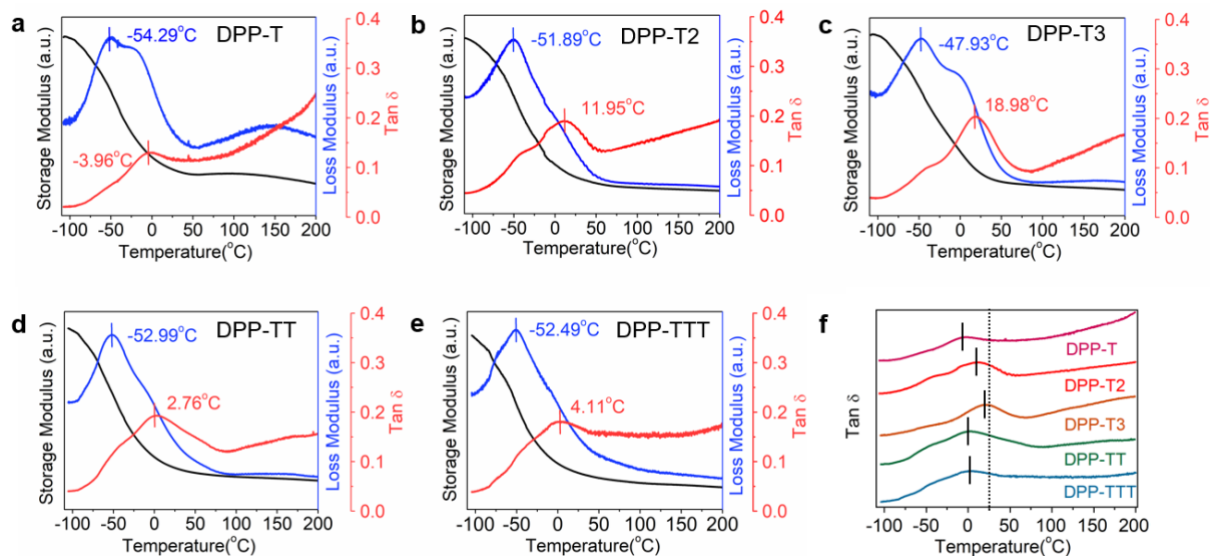
Figure 2. Viscoelastic property of DPP polymers measured by DMA. The storage modulus, loss modulus and tan δ are plotted for (a) DPP-T (b) DPP-T2 (c) DPP-T3 (d) DPP-TT (e) DPP-TTT. The backbone T_g is marked on the transition peak of tan δ. The side-chain T_g is marked on the transition peak of loss modulus. (f) Summary of tan δ curve for five DPP polymers. The vertical dotted line in figure (f) represents the room temperature, or 25 °C.
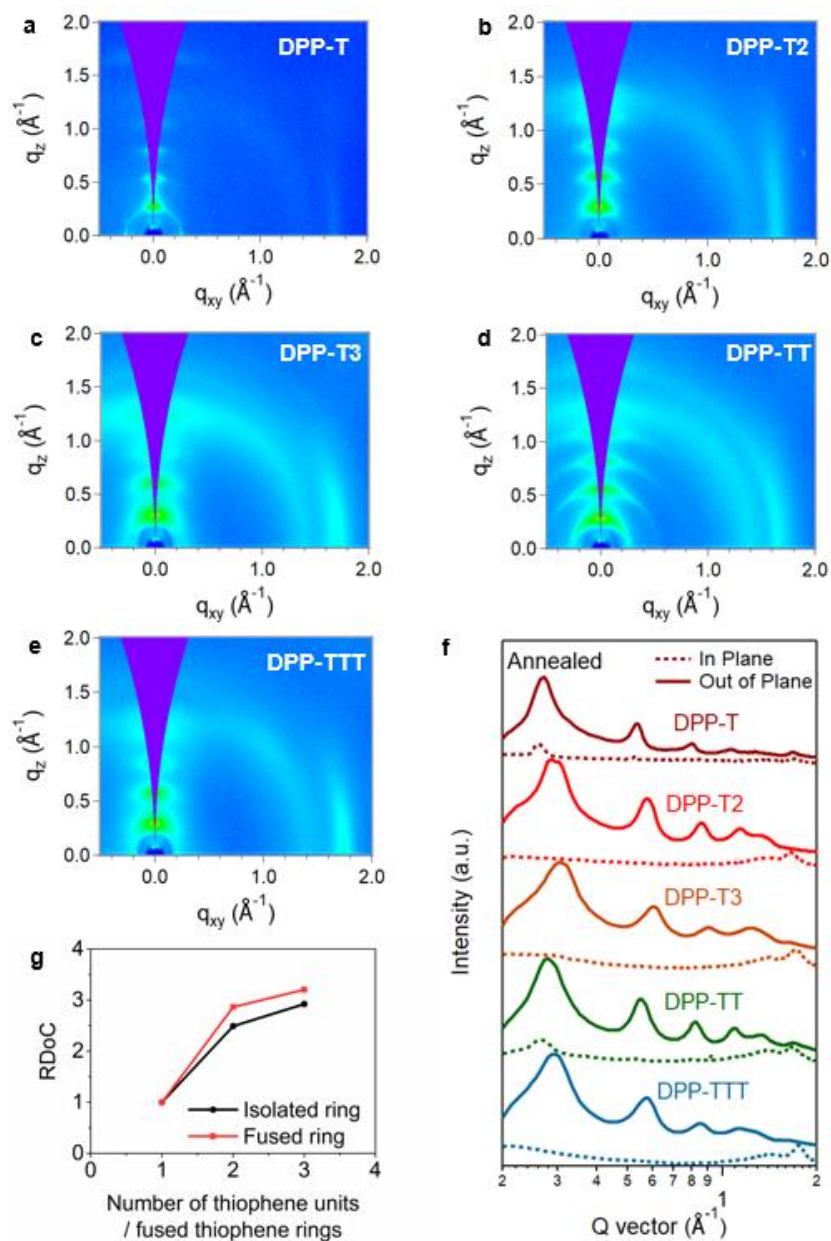
Figure 3. 2D GIWAXS pattern of DPP-based polymers after annealing. (a) DPP-T, (b) DPP-T2, (c) DPP-T3, (d) DPP-TT, (e) DPP-TTT. (f) 1D line-cut profiles in both in-plane direction (dotted line) and out-of-plane direction (solid line). (g) RDoC for different polymers with isolated rings (black line) and fused rings (red).
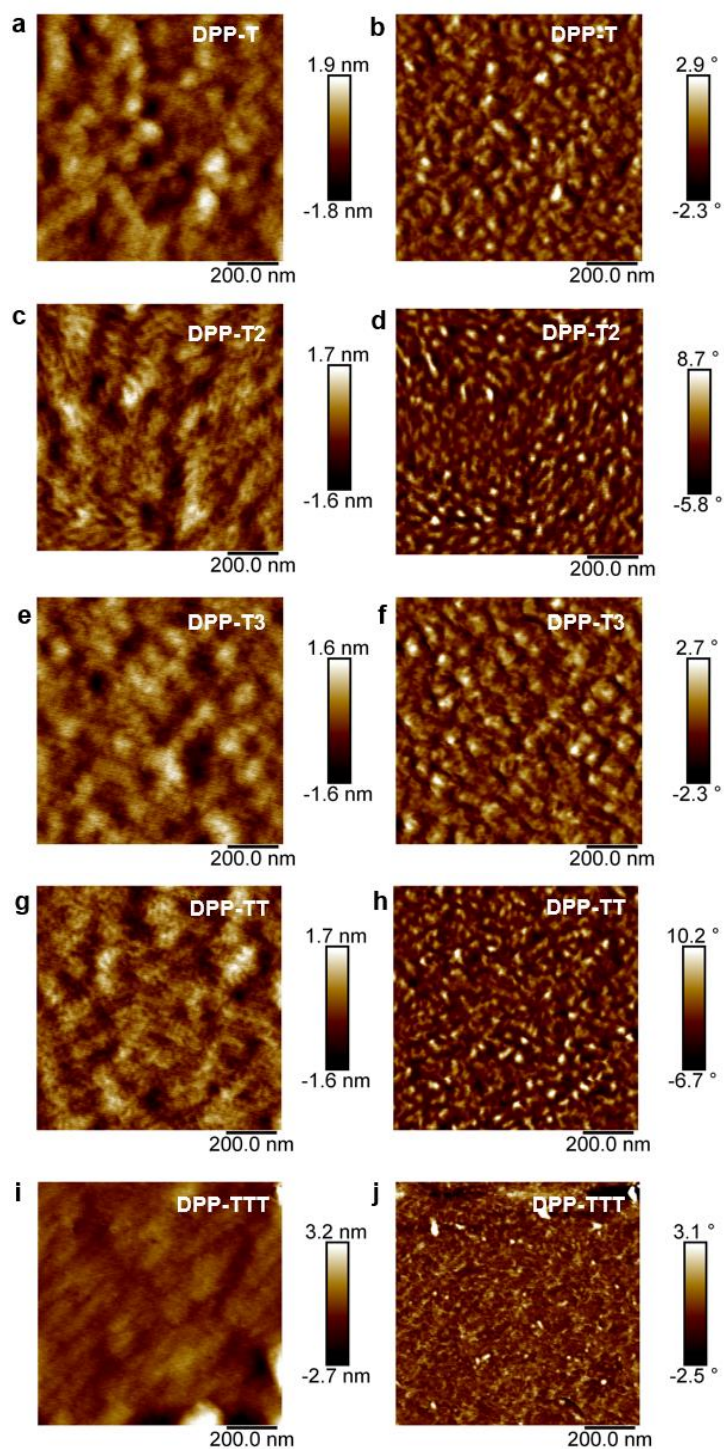
Figure 4. AFM images for annealed polymer films (a,b) DPP-T, (c,d) DPP-T2, (e,f) DPP-T3, (g,h) DPP-TT and (i,j) DPP-TTT. (a, c, e, g, i) are height images, (b, d, f, h, j) are phase images.
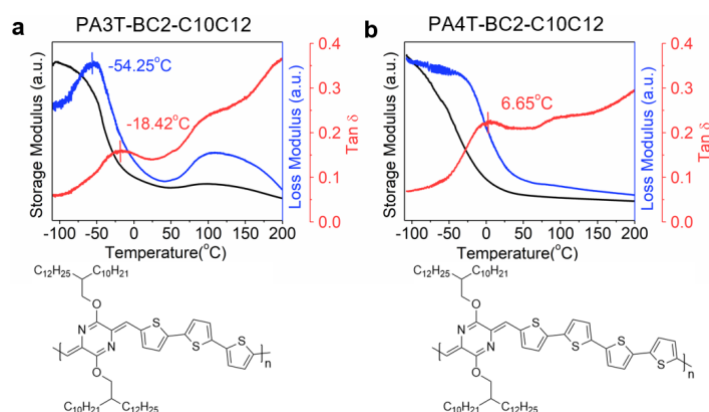
Figure 5. Chemical structures and DMA results for (a) PA3T-BC2-C10C12 and (b) PA4T-BC2-C10C12.
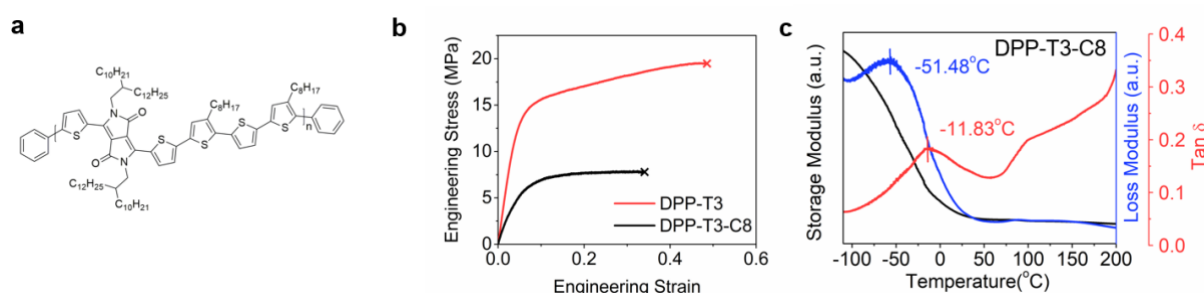
Figure 6. (a) Design of the new DPP-T3-C8 polymer with additional alkyl side chain. (b) Stress-strain curve of the DPP-T3-C8 polymer plotted with the same polymer without side chain. (c) DMA result of DPP-T3-C8 polymer.

Table 1. Physical properties of DPP polymers

Polymer	M_n (kDa) [a]	$Đ_w$ [b]	Side chain T_g (°C) [c]	Backbone T_g (°C) [d]	Backbone T_g (°C) [e]	Elastic modulus (MPa) [f]	Crack onset strain [f]
DPP-T	47	2.83	-54.29	-3.96	-11	173 ± 10	0.53 ± 0.20
DPP-T2	44	3.96	-51.89	11.95	17	281 ± 9	0.44 ± 0.09
DPP-T3	27	3.18	-47.93	18.98	19	319 ± 49	0.44 ± 0.10
DPP-TT	51	3.62	-52.99	2.76	3.5	400 ± 41	0.16 ± 0.03
DPP-TTT	26	3.69	-52.49	4.11	22	480 ± 40	0.03 ± 0.01

[a] Number-average molecular weight measured by high temperature GPC using trichlorobenzene as eluent at 170 °C. [b] Weight dispersity. [c] Obtained from peak of the loss modulus by DMA. [d] Obtained from the peak of tan δ plot in DMA. [e] Obtained from AC-chip calorimetry on thin film sample. Note that different T_g is expected due to different probing methods between DMA and calorimetry techniques. [f] Obtained from pseudo-free standing tensile test.

Table 2. Crystallographic parameters for DPP polymers

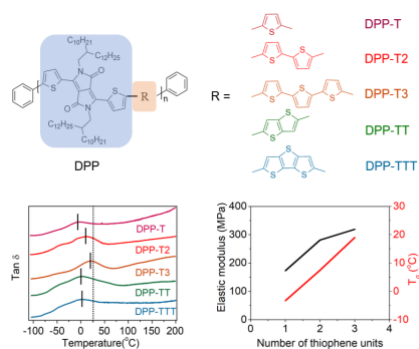| Polymer	Thermal treatment	Lamellar spacing (Å)	Lamellar peak FWHM (Å^{-1})	π-π spacing (Å)	π-π peak FWHM (Å^{-1})
DPP-T	As cast	22.20	0.1106	3.72	0.1799
	Annealed	23.44	0.0249	3.74	0.1315
DPP-T2	As cast	21.89	0.0550	3.74	0.1740
	Annealed	22.20	0.0250	3.77	0.1550
DPP-T3	As cast	20.53	0.0882	3.63	0.2362
	Annealed	20.67	0.0470	3.66	0.1583
DPP-TT	As cast	22.28	0.0519	3.69	0.2331
	Annealed	22.60	0.0367	3.78	0.1194
DPP-TTT	As cast	21.67	0.0833	3.60	0.1397
	Annealed	21.67	0.0430	3.59	0.1233

Trend: This paper investigates the effect of isolated/fused thiophene units on the thermomechanical properties of donor-acceptor conjugated polymers. In DPP-based polymers, it is noticed that thiophene units in the main chain structure serve as the anti-plasticizer, which increase the stiffness and glass transition temperature of polymer chains. This trend is also observed in another conjugated system, and later helps to develop a much softer conjugated polymer.

Keyword: thermomechanical property, conjugated polymer, structure-property relationship

Critical Role of Electron-Donating Thiophene Group on the Thermomechanical Property of Donor-Acceptor Semiconducting Polymers

*Song Zhang, Michael U. Ocheje, Lifeng Huang, Luke Galuska, Zhiqiang Cao, Shaochuan Luo, Dakota Ehlenberg, Renée Goodman, Dongshan Zhou, Yi Liu, Yu-Cheng Chiu, Jason D. Azoulay, Simon Rondeau-Gagné, * and Xiaodan Gu ***

ToC figure